References

[1] "Development and Demonstration of Criteria for Liquid Fluorine Feed System Component," CR-72063, Oct. 1967, McDonnell Douglas Astronautics Co., Huntington Beach, Calif.

[2] Endicott, D. L., "Development and Demonstration of Criteria for Liquid Fluorine Feed System Components," CR-72543, June 1969, McDonnell Douglas Astronautics Co., Huntington Beach, Calif.

[3] *Fluorine Systems Handbook,* NASA CR-72064, July 1967, McDonnell Douglas Astronautics Co., Huntington Beach, Calif.

Injector Design Criteria Using Noncircular Orifice Geometry

R. M. McHale,* W. H. Nurick,† and S. D. Clapp‡
Rocketdyne/North American Rockwell Corporation, Canoga Park, Calif.

THE most commonly used rocket engine injector designs in existence today employ circular orifices. However, with the advent of new fabrication techniques, noncircular orifices can now be produced with relative ease, and it is appropriate to evaluate their possible advantages. This Note presents experimental data on single-element cold-flow spray patterns evaluation and predicted performance differences among several noncircular and circular orifice configurations.

In the experimental technique employed, molten wax is used as one propellant simulant and hot water as the other. The spray of wax and water emanating from an injector is allowed to flow through the air for a time sufficient to allow the wax droplets to freeze. The frozen wax droplets are then caught on a platform, washed down into a particle catch basin, dried, weighed, and segregated by sieving.

Mixing efficiency of the injector elements was measured by collecting the spray from the element while flowing water and trichloroethylene. These fluids are immiscible. The spray is collected through an 841-tube matrix in separate glass tubes,

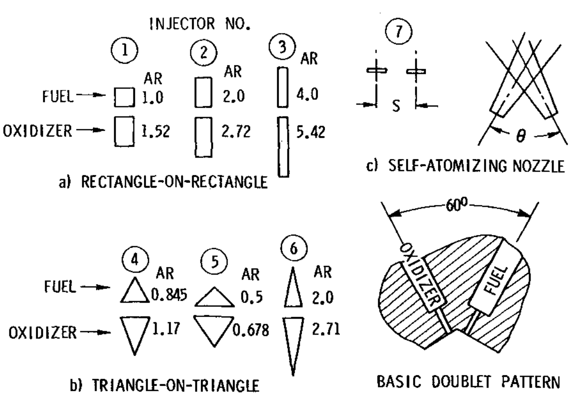

Fig. 1 Summary of injector patterns.

Received July 24, 1970; revision received September 8, 1970. Sponsored by NASA Manned Spacecraft Center, Houston, under initial Contract NAS9-9528; the NASA Technical Manager is M. Lausten.

* Member of Technical Staff.

† Member of Technical Staff. Member AIAA.

‡ Program Manager, Advanced Propulsion Technology. Member AIAA.

and the mixture ratio in each tube is recorded. The injectors are mounted 3 in. above the collection matrix.

Injector elements tested (Fig. 1) were unlike-impinging doublets and self-atomizing nozzles. In addition, an unlike doublet with circular orifices was tested to establish a reference point for comparison. Rectangular and triangular patterns were designed at several orifice aspect ratios (AR = height/width ratio of an orifice). For the triangular and rectangular elements, the widths of the two orifices in a given doublet were equal, and θ, the included angle of impingement, was set at 60°. The self-atomizing orifices were tested over ranges of spacing and impingement angle as shown in Fig. 1.

Results and Discussion

Mixing results

Results of cold-flow mixing studies conducted with the unlike doublets are presented in Fig. 2. Mixing uniformity E_m is correlated with a momentum ratio term N. Mixture ratio distribution uniformity E_m originally developed by Rupe at JPL[1] is defined by Eq. (1);

$$E_m = 100\left[1 - \sum_i^N MF_i \frac{R - r_i}{R} - \sum_i^{\bar{N}} MF_i \frac{R - r_i}{R - 1}\right] \quad (1)$$

where MF_i = mass fraction in ith tube; R = over-all mass ratio, trichloroethylene/trichloroethylene and water; r_i = mass ratio in ith tube, trichloroethylene/trichloroethylene and water; N = number of tubes in which $r < R$; and $\bar{N}$ = number of tubes in which $r > R$. The momentum ratio term N is given by the expression[2]

$$N = [1 + (M_f/M_0)(D_0/D_f)]^{-1} \quad (2)$$

where M_f/M_0 = fuel-to-oxidizer momentum ratio, and D_0/D_f = oxidizer-to-fuel orifice hydraulic diameter ratio (4 × area/perimeter = hydraulic diameter).

Results presented in Fig. 2 for unlike doublets of the impinging-type show that mixture ratio uniformity optimizes at N = 0.5 for noncircular orifices. For the spray fan injector (orifice spacing = 1 in.), mixing optimizes at an impingement angle of 60° included. As noted in Fig. 2, the level of mixing varies with orifice aspect ratio as well as with N.

Drop size results

Figure 3 presents atomization data for the specific elements which produced the highest mixing levels (i.e., numbers 2 and 4). Mass median droplet diameter decreases as the relative velocity between injectant and environmental gas increases. For the impinging-type elements, the rectangles produce droplets which are slightly smaller than the triangles.

Comparison of spray characteristics for optimized elements

The determination of the optimum injector design requires that all elements be designed according to Eq. (2) with N

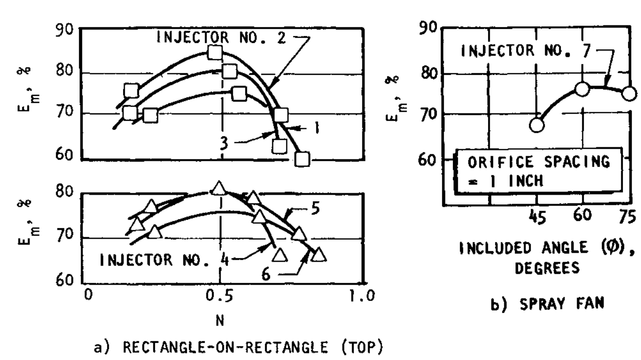

Fig. 2 Single-element mixing results.

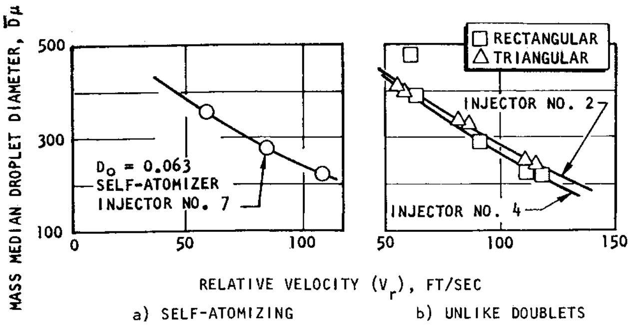

Fig. 3 Unlike doublet and spray fan atomization.

equal to 0.5. Introducing mixture ratio and the continuity equation, the variables in Eq. (2) can be separated from propellant physical variables, yielding

$$(A_0/A_f)D_0/D_f = (MR)^2\rho_f/\rho_0 \overset{\text{DEF}}{\equiv} K = 1.62 \text{ } N_2O_4/N_2H_4\text{-UDMH (50–50)} \quad (3)$$

where ρ = density and A = orifice area. All unlike-doublet injectors were designed according to Eq. (3). While the D_0/D_f for an element which yields high mixing uniformity is defined by Eq. (3), the optimum element AR is not. The determination of the optimum ARs can be accomplished as follows. First, from simple geometric considerations of A, AR, and D, the following expressions may be derived that relate oxidizer and fuel orifice AR to the given propellant combination:

$$\text{Rectangles:} \quad K(AR_f)^2/(AR_f + 1) = (AR_0)^2/(AR_0 + 1) \quad (4)$$

$$\text{Triangles:} \quad K(AR_f)^2/1 + (4AR_f^2 + 1)^2 = (AR_0)^2/(1 + 4AR_0^2 + 1)^2 \quad (5)$$

Therefore, there is a unique relationship between AR_f and AR_0. Secondly, E_m at $N = 0.5$ for each element design is plotted in Fig. 4 as a function of the fuel orifice AR. It can be seen that there is an optimum fuel orifice AR for each shape, and because of the relationships of Eqs. (4) and (5), there is a corresponding unique oxidizer orifice aspect ratio. The optimum designs for N_2O_4/N_2H_5-UDMH (50–50) are given in Fig. 4.

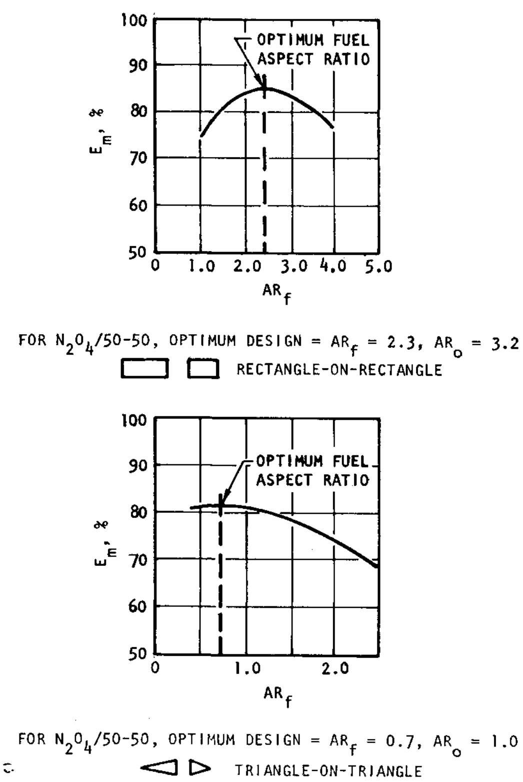

Fig. 4 Design criteria for unlike-doublet mixing.

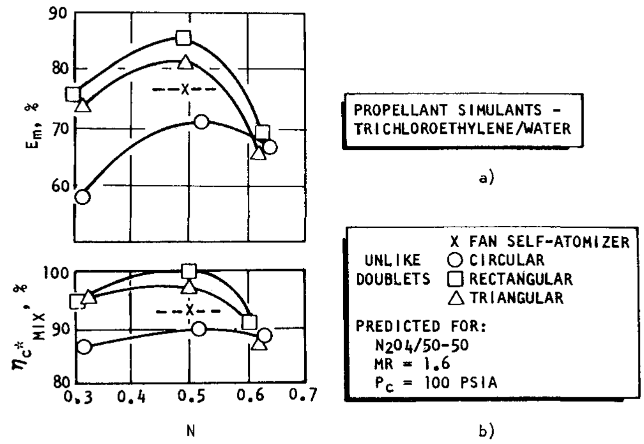

Fig. 5 Comparison of mixing characteristics of several optimized noncircular orifice elements with an optimized conventional circular orifice element.

In Fig. 5a, the configuration closest to the optimum for the noncircular orifice unlike-doublet and self-atomizing element are compared to those of an optimized single unlike-doublet element with circular orifices. The noncircular orifice elements result in more uniformly mixed sprays than the circular element. These cold-flow results were input into the Rocketdyne mixing limited stream tube model program[3] and η_c*, mixing determined for the N_2O_4/50–50 propellant combination. The results are presented in Fig. 5b. As with the uniformity of the sprays, the noncircular orifice elements result in higher c^* mixing limited combustion efficiency than the circular element. The rectangular element results in about a 7% increase, and the atomizing element results in about 2% increase.

To apply the drop size results obtained with wax to predict performance within a rocket engine, the influence on drop size of the difference in physical properties between a given propellant and wax must be taken into account. In addition, the gas velocity resulting from combustion within the combustion chamber must be considered in the determination of resulting spray drop size.[4]

As in Ref. 3, the droplet diameter corrections for physical properties for N_2O_4/50–50 are

$$\bar{D}_{\text{ox}} = 0.528\bar{D}_{\text{wax}} \qquad \bar{D}_{\text{fuel}} = 0.782\bar{D}_{\text{wax}} \quad (6)$$

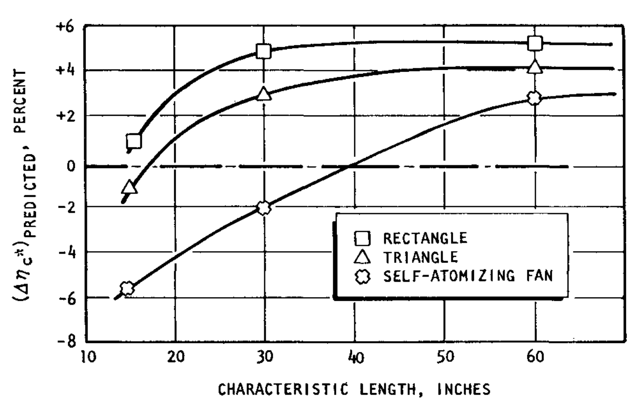

Fig. 6 Prediction of over-all performance differences between optimized single-element noncircular and circular orifice injectors for N_2O_4/50-50 and contraction ratio 4.0.

Table 1 Comparison of drop size for circular and noncircular orifices at engine operating conditions

Orifice type	D_{0z},[a] μ	D_f,[a] μ
Circular (unlike doublet)	43	65
Triangular (unlike doublet)	65	91
Rectangular (unlike doublet)	60	98
Self-atomizing	63	102

[a] At V_r — 200 fps; corrected for physical properties.

For rocket engine designs with contraction ratios of 3 to 4, the average combustion gas velocity acting on the spray fan is about 200 to 300 fps. For purposes of comparison, a relative velocity of 200 fps has been chosen ($\theta = 4.0$).

Drop sizes were computed by first determining the drop size for each element type from Fig. 3 at a relative velocity (V_r) of 200 fps and then applying the physical property correction shown in Eq. (6) for each propellant. The resulting drop sizes are shown in Table 1; the circular element has smaller drop sizes than noncircular elements.

To determine the overall predicted c^* efficiency, the mixing-limited c^* efficiency and the vaporization-rate-limited c^* efficiency are combined in the first-order approximation;

$$(\eta_{c^*})_{\text{predicted}} = (\eta_{c^*})_{\text{mixing}} \times (\eta_{c^*})_{\text{vaporization}} \tag{7}$$

The atomization and mixing results, shown in Table 1 and Fig. 5 were input into the mixing-limited and vaporization-rate-limited combustion models to predict the over-all c^* performance characteristics for both optimized circular and noncircular orifice elements. The results are shown in Fig. 6 in terms of $\Delta\eta_{c*}$ and characteristic chamber length (L^*). The $\Delta\eta_{c*}$, predicted is defined as

$$(\Delta\eta_{c^*})_{\text{predicted}} = (\eta_{c^*})_{\substack{\text{predicted}\\ \text{noncircular}}} - (\eta_{c^*})_{\substack{\text{predicted}\\ \text{circular}}} \tag{8}$$

Predictions were made for N_2O_4/50–50 and contraction ratio 4.0. The results show that the rectangular orifice unlike-doublet element will operate between 1 and 6% higher in c^* efficiency than the conventional circular unlike-doublet element over the range of L^* between 15 and 60 in. In addition, the triangular unlike doublet will perform about 1% lower than the circular element at an L^* of 15 in.; however, at increased L^*'s the triangular element performs at a higher level than the circular (4% at 60-in. L^*). The self-atomizing element performs about 6% lower than the circular unlike-doublet element at an L^* of 15 in., and 3% higher at an L^* of 60 in.

The contraction ratio 4.0 yields results that are rather pessimistic with respect to the benefits which could be derived from noncircular elements. Higher combustion gas velocities produced by lower contraction ratios would decrease the drop sizes for the various elements and consequently, the performances of the noncircular elements would be greatly improved.

Conclusions

Program results to date have indicated that noncircular orifice configurations can, under some conditions, produce performance characteristics that are superior to those of the conventional circular shape. This is especially true with respect to propellant mixing. The correlations developed suggest that for liquid-liquid propellants, it is possible to retain the simple unlike-doublet element configuration for any propellant combination and operating mixture ratio if noncircular orifices are used, since these designs can accommodate the density and flowrates involved by appropriate adjustments in aspect ratio keeping one side of each rectangule equal. Therefore, noncircular orifice elements supply the desired mixing and atomization levels while maintainng the simplicity of an unlike doublet.

References

[1] Rupe, J. H., "A Correlation Between the Dynamic Properties of a Pair of Impinging Streams and the Uniformity of Mixture-Ratio Distribution in the Resulting Spray," Progress Rept. 20-209, March 1956, Jet Propulsion Lab., Pasadena, Calif.

[2] Rupe, J. H., "The Liquid Phase Mixing of a Pair of Impinging Streams," Progress Rept. 20-195, Aug. 1955, Jet Propulsion Lab., Pasadena, Calif.

[3] Dickerson, R. et al., "Correlation of Spray Injector Parameters with Rocket Engine Performance," R-7499 (AFRPL-TR-68-147), June 1968, Rocketdyne/North American Rockwell Corp., Canoga Park, Calif.

[4] Falk, A. Y. et al., "Space Storable Propellant Performance Study, Final Report," R-7677 (NASA CR-72487), Nov. 1968, Rocketdyne/North American Rockwell Corp., Canoga Park, Calif.

Disintegration of a Supersonic Jet Impinging Normally on a Flat Plate

T. NAKATOGAWA,* M. HIRATA,† AND Y. KUKITA*
University of Tokyo, Tokyo, Japan

Nomenclature

$b_{1/2}$ = collision radius $\{b_{1/2} = r_{[p-p_\infty = \frac{1}{2}(p_s - p_\infty)]}\}$
D = nozzle exit diameter
H = distance between nozzle exit and flat plate
p = static pressure
p_s = stagnation pressure on flat plate
p_∞ = ambient pressure
r = radial coordinate

Introduction

THERE have been many studies of the structure of a supersonic freejet in relation to jet noise. In the case of a highly underexpanded freejet, very strong directional sound called "screech" is generated. It was shown that the highly under-expanded jet disintegrates when this screech is generated. Powell[1] first described and explained this disintegration in terms of a mechanism involving the pattern of shock waves. But in this Note, it is proved that, for the case of a supersonic jet of almost correct expansion (nozzle exit Mach number 1.6) impinging normally on a flat surface, similar disintegration also occurs with strong screech when the normal shock wave in front of the flat surface is in a decelerating region of the jet.

Air was supplied continuously by a 10 *HP* compressor to a round Laval nozzle preheated to 175°C. The expansion in the nozzle was always checked by four static pressure taps at the nozzle wall during the experiments, and no odd change in pressure distribution was observed. The nozzle exit of the diameter D of 5.00 mm was located in the center of a brass disk baffle of 76.0 mm diam, that is, this nozzle had an acoustic reflector, as in the work of Glass,[2] normal to the nozzle axis. A square flat plate of 30-cm side-length is set normally to the jet axis as the jet impinging target at the

Received September 4, 1970.
* Graduate Student, Department of Mechanical Engineering.
† Professor, Department of Mechanical Engineering.